



Fluid-structure interaction analysis of a hypothetical core disruptive accident in LMFBRs

Chuang Liu*, Xiong Zhang, Ming-Wan Lu

Department of Engineering Mechanics, Tsinghua University, Beijing 100084, People's Republic of China

Received 9 August 2004; received in revised form 2 November 2004; accepted 4 November 2004

Abstract

To ensure safety, it is necessary to assess the integrity of a reactor vessel of liquid-metal fast breeder reactor (LMFBR) under HCDA. Several important problems for a fluid-structural interaction analysis of HCDA are discussed in the present paper. Various loading models of hypothetical core disruptive accident (HCDA) are compared and the polytropic processes of idea gas (PIIG) law is recommended. In order to define a limited total energy release, a “5% truncation criterion” is suggested. The relationship of initial pressure of gas bubble and the total energy release is given. To track the moving interfaces and to avoid the severe mesh distortion an arbitrary Lagrangian–Eulerian (ALE) approach is adopted in the finite element modeling (FEM) analysis. Liquid separation and splash from a free surface are discussed. By using an elasticity solution under locally uniform pressure, two simplified analytical solutions for 3D and axi-symmetric case of the liquid impact pressure on roof slab are derived. An axi-symmetric finite elements code FRHCDA for fluid-structure interaction analysis of hypothetical core disruptive accident in LMFBR is developed. The CONT benchmark problem is calculated. The numerical results agree well with those from published papers.

© 2004 Elsevier B.V. All rights reserved.

1. Introduction

The Liquid-metal fast breeder reactor (LMFBR) is a high-efficient nuclear reactor. Many fast reactors were constructed in the world, such as in the US, France, Russia, the UK, Japan, Germany and India. China pays

high attention to the development of nuclear energy utilization. As the first step, several units of PWRs have been built in China. For efficient utilization of uranium resources, research on LMFBRs was also started. To ensure safety, it is necessary to assess the integrity of the reactor vessel of a LMFBR under a hypothetical core disruptive accident (HCDA), which is the most serious accident in LMFBRs. The HCDA starts when the decay heat cannot be removed. Then the core temperature rises. When reaching the temperature of Na-evaporation, a void is formed. Here, the fast neutrons

* Corresponding author. Tel.: +86 10 62782078;
fax: +86 10 62781824.

E-mail addresses: lch98@mails.tsinghua.edu.cn,
liuchuang@tsinghua.org.cn (C. Liu).

are not slowed down. Since the void coefficient is very positive the reactor power increases very rapidly. Thus a high-pressure gas bubble quickly forms and explosively expands. The explosive wave propagates radially and leads to overloading the core surrounding structures (reflectors, shields, etc.) and the reactor vessel. Moreover, the explosive gas bubble thrusts the liquid sodium upwards to compress and push aside the argon cover gas and impacts on the roof slab. If excessive plastic deformation is obtained in the reactor vessel or in the roof slab during hypothetical core disruptive accident, the safety of the assessed reactor is unacceptable.

Fluid-structure interaction analysis is the key of structural safety assessment of HCDA in LMFBRs. Many papers on this topic have been published in a series of proceedings of SMiRT conferences, in the issues of the Journal of Nuclear Engineering and Design, and in a special issue on FBR of the Journal of Nuclear Technology (Han, 1980), etc.

2. Modeling of HCDA analysis

Different from PWRs the main reactor vessel of a LMFBR is a thin-walled vessel with a thick roof slab. It contains a reactor core and several internal structures, such as the core support structure, the radial shield, etc. The remainder space in the main vessel is filled by three fluid components: (1) liquid sodium as a coolant, (2) inertial argon blanket as an isolator, (3) a high-pressure gas bubble as a loading resource. The structural components are modeled by the elasto-plastic finite elements and the fluid components are modeled by viscous incompressible fluid finite elements.

An important problem is how to create a loading model simulating the HCDA process. An exact simulation of HCDA process requires a complicated multi-discipline analysis involving nuclear physics, thermodynamics and fluid dynamics, etc. Such a complete coupling analysis is yet impossible for us. Since the goal of this HCDA analysis is to ensure the integrity of the reactor vessel under HCDA, but not to simulate the HCDA process in detail, so most researches assumed the following loading models for low-density explosive charges.

- (1) JWL (Jones–Wilkinson–Lee) equation of state (Kury et al., 1965; Hoskin and Lancefield, 1978):

$$p = A \left(1 - \frac{W}{R_1 V} \right) e^{-R_1 V} + B \left(1 - \frac{W}{R_2 V} \right) e^{-R_2 V} + \frac{W}{V} (E - E_1) \quad (1)$$

$$E_1 = A \left(\frac{1}{W} - \frac{1}{R_1} \right) e^{-R_1} + B \left(\frac{1}{W} - \frac{1}{R_2} \right) e^{-R_2}$$

where p is the pressure, V' the relative volume, E the internal energy, W the total energy release during the HCDA process and A, B, R_1, R_2 are the physical constants. The expression of E_1 comes from the initial condition: $p = 0$ and $V' = 1, E = 0$.

- (2) The polytropic processes of ideal gas (PPIG) law (Cengel and Boles, 2002, p. 135):

$$pV^n = \text{const} \quad (2)$$

where p and V denotes the pressure and volume respectively and n is a material constant.

- (3) Argonne National Laboratory (ANL) equation of state (Wang, 1980):

$$p = 0.92453 \frac{E}{V'} + \frac{0.054925}{V'^{3.09303}} \quad (3)$$

- (4) Generalized Perfect Gas (GPG) law (Wenger and Smith, 1987):

$$p = p_0 \left(\frac{1 - \beta}{V' - \beta} \right)^\gamma \quad (4)$$

where the constants are chosen to be $\beta = 0.279175$ and $\gamma = 1.27943$.

We have compared the above loading models. The results are shown in Figs. 1 and 2. Following conclusions can be drawn from the comparison:

- (1) The PPIG law is the most flexible loading model. It can be applied to various loading cases. When the value of n increases, the pressure drops rapidly and the energy release decreases.
- (2) When $n = 1$, the PPIG law is closer to the Jones–Wilkinson–Lee equation of state.
- (3) Although for an ideal gas the parameter n in PPIG law is limited to be equal to or less than 1.0, but Fig. 1 and Fig. 2 show that if generalizing the law to take $n = 1.4$, it is closer to the ANL equation of state and the GPG law.

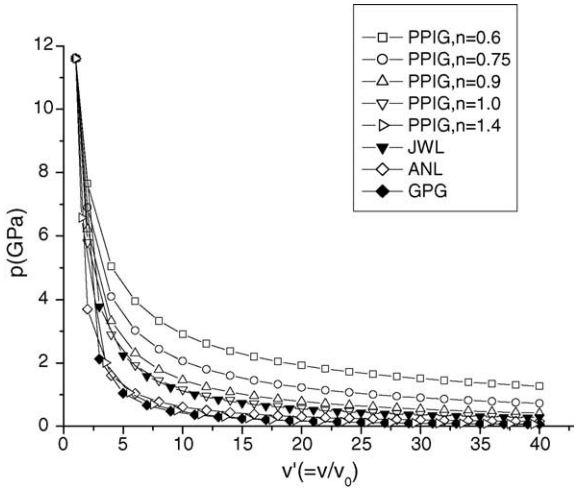


Fig. 1. Comparison of loading models: pressure vs. relative volume.

In the PPIG loading model the parameter n represents the rate of change, the initial pressure p_0 and the initial volume V_0 represent the magnitude of work and are related to the total energy release W .

Consider the polytropic processes of $n = 1$, set the $\text{const} = C$ in the right-hand of Eq. (2), we get the energy release during the expansion from V_0 to V_2 (here V_0 is the initial volume of gas bubble):

$$w = \int_{V_0}^{V_2} p dV = \int_{V_0}^{V_2} \frac{C}{V} dV = C \ln V \Big|_{V_0}^{V_2} \quad (5)$$

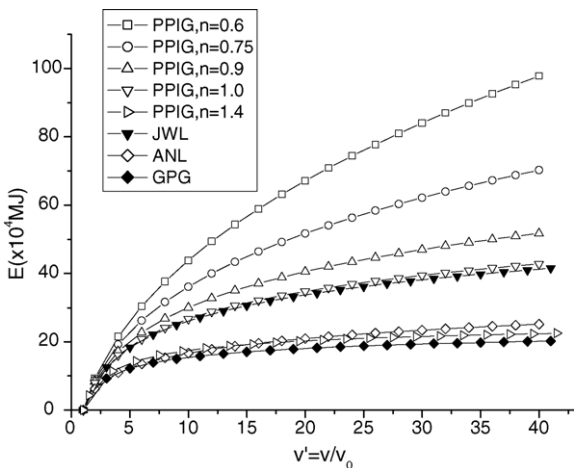


Fig. 2. Comparison of loading models: energy release vs. relative volume.

Table 1
Rated power and total energy release of several FBRs

Name of FBR	Rated power (MW)	Total energy release (MJ)
Phoenix (France)	600	150, 300, 500
Superphoenix (France)	3000	800
FFTF (USA)	400	150
CRBR (USA)	975	661
SNR300 (Germany)	700	370
PFBR (India)	500	200

Eq. (5) means that if $V_2 \rightarrow \infty$, i.e. the gas bubble expands infinitely, the energy release w will also tend to infinite. In order to define a limited total energy release W , we suggest a “5% truncation criterion”—if the volume of the gas bubble expands two times from $V_2 = \eta V_0$ to $2V_2$, the energy release during this expansion is equal to 5% of that during the expansion from V_0 to V_2 , then the energy release w during the expansion from V_0 to V_2 is defined as the total energy release W . From

$$\frac{C \ln(2V_2/V_2)}{C \ln(V_2/V_0)} = \frac{\ln 2}{\ln \eta} = 0.05 \quad (6)$$

we get the parameter η corresponding to the 5% truncation criterion to be equal to $2^{10} \approx 10^6$, so the total energy release W is equal to the pressure work during the million times expansion of the gas bubble from its initial state.

From Eqs. (2) and (5) we have $C = p_0 V_0 = W/\ln \eta$, thus the relationship of initial pressure p_0 and total energy release W is

$$p_0 = \frac{W}{V_0} \ln \eta = \frac{W}{13.86 V_0} \quad (7)$$

For the polytropic processes of $n < 1.0$, we get

$$W = \int_{V_0}^{V_2} p dV = \int_{V_0}^{V_2} \frac{C}{V^n} dV = \frac{C}{1-n} V^{1-n} \Big|_{V_0}^{V_2} \quad (8)$$

and

$$p_0 = \frac{(1-n)W}{(\eta^{1-n} - 1)V_0} \quad (9)$$

Normally the magnitude of a HCDA is estimated by a ratio of the total energy release W and the rated power of the LMFBR. With accumulation of experiences, the ratio is selected less and less. It decreases from 10 s in the 1960s to 0.5 s in the 1980s. Several examples are listed in Table 1.

3. Tracking of moving interface

There exist several moving interfaces in the fluid-structure interaction analysis of HCDA in a LMFBR: (1) interface of the high-pressure gas bubble and the liquid sodium, which enlarges rapidly along with the expansion of the gas bubble; (2) interface of the liquid sodium and the inertial argon blanket, which is pushed ahead by the expanding gas bubble; (3) interface of the fluid and the structural components, which occurs tangential sliding during the fluid movement.

For numerical analysis of fluid problems there are two basic approaches: one is the Eulerian approach, which selects a reference coordinate fixed in the space, another is the Lagrangian approach, which selects a reference coordinate moving with the body together. The methods for tracking the moving interface in the Eulerian approach and in the Lagrangian approach are called “front capturing” and “front tracking”, respectively (Jiang, 1998). The former includes the marker-and-cell (MAC) method suggested by Harlow and Welch (1965), the volumes of fluid (VOF) method proposed by Hirt and Nichols (1981) and the level set method (LSM) published by Zhu and Sethian (1992), etc. The MAC uses a lot of massless mark particles traveling with the fluid to trace the fluids and the interface. Distinction of two different fluids is either with mark particles or not. The VOF and the LSM modify the MAC method by replacing the discrete marker particles with a continuous field variable—a color function or level set function. These functions assign a unique constant (color) to each fluid. At fluid interface this color function has a sharp gradient. The difficulty of the front capturing methods is how to identify the interface accurately and to impose the interface conditions. The latter is often used in the FEM, which updates the computational meshes frequently to coincide the mesh sides with the moving interface. The difficulty of the front tracking methods occurs when the meshes are distorted severely.

Compared to the above methods the arbitrary-Lagrange–Euler (ALE) method (Noh, 1964) is more general and more flexible to deal with the moving interface problem. In the ALE method we can specify such a movement of meshes: at the interface the mesh side moves with material particles together (reduce to the Lagrangian approach) to track the moving interface. At a distance from the interface the meshes are fixed in

the space (reduce to the Eulerian approach) to reduce the number of updated meshes, and in the intermediate zone the meshes move independently, neither stuck on the material particles nor fixed in space, to avoid severe distortion of meshes.

The earlier numerical analyses of HCDA normally adopt the Lagrangian approach or the Eulerian approach. For instance, the computer codes REXCO-HEP, REXCO-HT, ASTARTE, ARES and EURDYN select the Lagrangian approach (Wang, 1980); the computer codes ICECO, PISCES2DELK, CASSIOPEE and SEURBNUK selected the Eulerian approach (Wang, 1980, and Wayne, 1980). Several analyses adopt the ALE formulation, such as the computer codes ALICE, NEPTUNE, STRAW, REXALE-3D and CEA/DMT PLEXUS (Wang, 1980; Han, 1980; Lepareux et al., 1993). Recent researches or the resent versions of the above mentioned codes tend to adopt the ALE formulation. Robbe et al. (2003) reported a detailed numerical simulation of HCDA in MARA 10 experimental test, a 1/30-scale model of the Superphoenix reactor, by an ALE-type code EUROPLEXUS. In this paper, the ALE formulation is also adopted.

The ALE formulation of Navier–Stokes equation of a viscous incompressible fluid is:

$$\rho \left(\frac{d\mathbf{v}}{dt} + (\mathbf{v} - \mathbf{v}_m) \cdot \nabla \mathbf{v} \right) - \nabla \cdot \boldsymbol{\sigma} = \rho \mathbf{f} \quad \text{in } \Omega \times (0, T) \quad (10)$$

incompressible condition is presented with

$$\nabla \cdot \mathbf{v} = 0 \quad \text{in } \Omega \times (0, T) \quad (11)$$

stress and strain expressions are:

$$\boldsymbol{\sigma} = -p\mathbf{I} + 2\mu\boldsymbol{\varepsilon}(\mathbf{v}) \quad (12)$$

$$\boldsymbol{\varepsilon}(\mathbf{v}) = \frac{1}{2}(\nabla \mathbf{v} + (\nabla \mathbf{v})^T) \quad (13)$$

where $d\mathbf{v}/dt$ is a mesh-derivative of material velocity, \mathbf{v}_m the mesh-velocity, p the pressure in the fluid, \mathbf{f} the force per unit mass, ρ the fluid density, μ the kinematic viscosity, and $\boldsymbol{\sigma}$ and $\boldsymbol{\varepsilon}$ are the stress and the strain tensor, respectively.

The boundary conditions for the velocity and the surface forces are:

$$\mathbf{v} = \mathbf{g} \quad \text{on } \Gamma_g \quad (14)$$

$$\mathbf{n} \cdot \boldsymbol{\sigma} = \mathbf{h} \quad \text{on } \Gamma_h \tag{15}$$

The initial conditions are:

$$\begin{aligned} \mathbf{v}(\mathbf{x}, 0) &= \mathbf{v}_0 \\ \nabla \cdot \mathbf{v}_0 &= 0 \end{aligned} \tag{16}$$

Based on the above mentioned equations and conditions, the Galerkin integral method is:

$$\begin{aligned} \int_{\Omega_e} \delta \mathbf{v} \left[\rho \left(\frac{d\mathbf{v}}{dt} + (\mathbf{v} - \mathbf{v}_m) \cdot \nabla \mathbf{v} \right) - \nabla \cdot \boldsymbol{\sigma} - \rho \mathbf{f} \right] d\Omega \\ - \int_{\Gamma_{he}} \delta \mathbf{v} [\mathbf{n} \cdot \boldsymbol{\sigma} - \mathbf{h}] d\Gamma = 0 \end{aligned} \tag{17}$$

The ALE formulations for finite element method are obtained:

$$\mathbf{M} + \mathbf{K}\mathbf{v} + \mathbf{N}(\mathbf{v} - \mathbf{v}_m) - \mathbf{G}\mathbf{p} = \mathbf{F} \tag{18}$$

$$\mathbf{G}^T \mathbf{v} = 0 \tag{19}$$

where \mathbf{M} is mass matrix, \mathbf{K} the viscosity matrix, \mathbf{N} the non-linear vector of convection force, \mathbf{G} the gradient operator and \mathbf{F} is the force vector. Their detailed expressions are as follows.

$$\mathbf{M} = \sum_{e=1}^{N_e} \int_{\Omega_e} \rho \mathbf{N}_v^T \mathbf{N}_v d\Omega \tag{20}$$

$$\mathbf{K} = \sum_{e=1}^{N_e} \int_{\Omega_e} \mu \mathbf{B}_v^T D \mathbf{B}_v d\Omega \tag{21}$$

$$\mathbf{N} = \sum_{e=1}^{N_e} \int_{\Omega_e} \rho \mathbf{N}_v^T [\mathbf{N}_v (\mathbf{v} - \mathbf{v}_m) \cdot \nabla] \mathbf{N}_v d\Omega \tag{22}$$

$$\mathbf{G} = \sum_{e=1}^{N_e} \int_{\Omega_e} \mathbf{N}_v^T (\nabla \cdot \mathbf{N}_p) d\Omega \tag{23}$$

$$\mathbf{F} = \sum_{e=1}^{N_e} \int_{\Omega_e} \rho \mathbf{N}_v^T f d\Omega + \sum_{e=1}^{N_h} \int_{\Gamma_{he}} \mathbf{N}_v^T \mathbf{h} d\Gamma \tag{24}$$

$$\mathbf{D} = \begin{bmatrix} 1 & 0 & 0 & 0 & 0 & 0 \\ 0 & 1 & 0 & 0 & 0 & 0 \\ 0 & 0 & 1 & 0 & 0 & 0 \\ 0 & 0 & 0 & 0.5 & 0 & 0 \\ 0 & 0 & 0 & 0 & 0.5 & 0 \\ 0 & 0 & 0 & 0 & 0 & 0.5 \end{bmatrix} \tag{25}$$

$$\mathbf{B}_v = \begin{bmatrix} \frac{\partial}{\partial x} & 0 & 0 & 0 & \frac{\partial}{\partial z} & \frac{\partial}{\partial y} \\ 0 & \frac{\partial}{\partial y} & 0 & \frac{\partial}{\partial z} & 0 & \frac{\partial}{\partial x} \\ 0 & 0 & \frac{\partial}{\partial z} & \frac{\partial}{\partial y} & \frac{\partial}{\partial x} & 0 \end{bmatrix}^T \mathbf{N}_v \tag{26}$$

where \mathbf{N}_v and \mathbf{N}_p is shape function matrix of the velocity field and the pressure field, respectively, and N_h is the number of elements on the boundary Γ_h .

4. Impact of splashing liquid on the roof

The explosive load of a high-pressure gas bubble transfers to the wall of the reactor vessel by two ways: (1) propagation of pressure wave through the liquid sodium and argon blanket, which can be simulated well by the fluid-structural coupling analysis of FEM and (2) impact of splashed liquid sodium on the roof slab, which is discussed in detail as follows.

4.1. Separation criterion of liquid

Since the liquid cannot be subjected to extension, if the normal stress at a point in liquid is greater than or equal to zero

$$\boldsymbol{\sigma} \geq 0 \tag{27}$$

a separated infinitesimal free surface will appear immediately. During an explosion under liquid the infinitesimal free surfaces extend and connect each other to form a macro free surface. When a part of the liquid near an original free surface is surrounded by the original free surface and the separated free surface, then the liquid part will be separated from the whole liquid and splash off. For a severe explosion the effect of surface tension on the free surface can be neglected.

4.2. Splashing trace of liquid part

By using Newton's second law to the mass center, we get a motion equation of a separated liquid part:

$$m\mathbf{a} = \mathbf{F} \quad (28)$$

where m denotes mass of the liquid part, \mathbf{a} is acceleration of the mass center, \mathbf{F} is a gravitational force, the air resistance is ignored. Solution of Eq. (28) is a projectile motion

$$\mathbf{v}_t = \mathbf{v}_0 + \mathbf{g}t \quad (29)$$

where \mathbf{v}_t is current velocity, \mathbf{v}_0 is initial velocity, which is equal to a velocity of the liquid part at the moment just separated from the whole liquid, \mathbf{g} is the acceleration of gravity, t is the time of liquid flight.

By integrate in Eq. (29), we get the flying height of the splashing liquid:

$$h = \frac{v'_0}{2g} \quad (30)$$

where v' is the vertical component of the initial separated velocity, if h is equal to or larger than the vertical distance between free surface of liquid sodium and roof slab, the splashing liquid part will impact on the roof slab.

4.3. Impact pressure on roof slab

A simplified analytical solution of the impact pressure on the roof slab can be obtained by using an elasticity solution under locally uniform pressure.

Suppose the impact pressure q is uniformly distributed over a circular area of radius a . Based on the Boussinesq solution of a semi-infinite solid loaded by a concentrated force P at the origin, the deflection of the boundary plane $z=0$ in the direction of the load is:

$$(u_z)_{z=0} = \frac{P(1-\nu^2)}{\pi E_e r} \quad (31)$$

where E_e and ν are the Young's modulus and the Poisson's ratio, respectively. Consider a point M within the loaded area, its deflection produced by a loaded element shown shaded in Fig. 3 can be obtained from Eq. (31), in which the concentrated load and the distance between M and loaded element are $qsdsd\psi$ and s instead of P and r , respectively. Then the total deflection

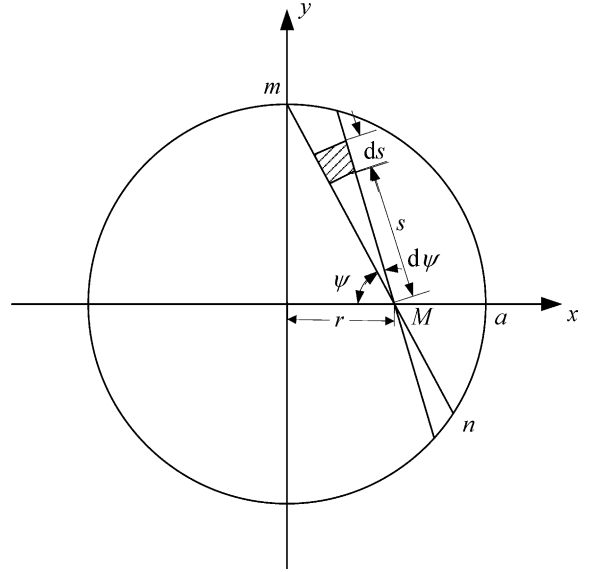


Fig. 3. Round area in 3D semi-infinite solid.

is

$$u_z = \frac{(1-\nu^2)q}{\pi E_e} \iint ds d\psi \quad (32)$$

After integration, the deflection at a certain point M in the circular loaded area is (Timoshenko and Goodier, 1970, p. 404):

$$u_z = \frac{4(1-\nu^2)qa}{\pi E_e} \int_0^{\frac{\pi}{2}} \sqrt{1 - \frac{r^2}{a^2} \sin^2 \psi} d\psi \quad (33)$$

The force acting on an element at M in polar coordinate is equal to:

$$dF = qr d\theta dr \quad (34)$$

From Eqs. (33) and (34) we have the total work done by the impact pressure distributed in the loaded area:

$$\begin{aligned} W &= \int u_z dF \\ &= \int_0^a \int_0^{2\pi} \int_0^{\frac{\pi}{2}} \frac{4(1-\nu^2)q^2 a}{\pi E_e} \\ &\quad \times \sqrt{1 - \frac{r^2}{a^2} \sin^2 \psi} d\psi d\theta dr \\ &= \frac{16(1-\nu^2)q^2 a^3}{3E_e} \end{aligned} \quad (35)$$

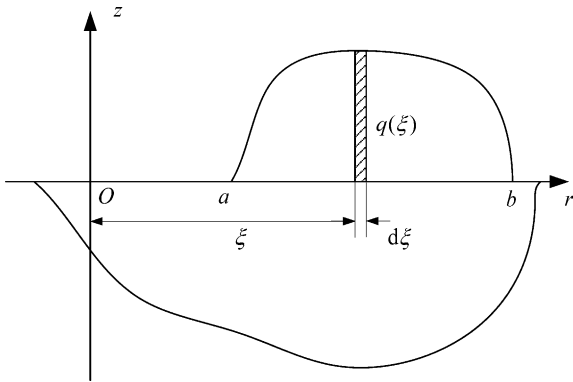


Fig. 4. Annular area in semi-infinite solid.

On the other hand, the mass and kinetic energy of a liquid sphere, which represents the splashing liquid part, are:

$$m = \rho \cdot \frac{4}{3}\pi a^3; \quad E = \frac{1}{2}mv^2 = \frac{2}{3}\rho\pi a^3 v^2 \quad (36)$$

For impact problems the energy is usually non-conservative. Suppose the rate of energy transfer is k ($0 \leq k \leq 1$), i.e. the impact work effecting on the roof slab is only k times of the kinetic energy of splashing liquid part, $W = kE$. Combine Eqs. (35) and (36), then the impact pressure q is obtained

$$q = v \sqrt{\frac{k\rho\pi E_e}{8(1-v^2)}} \quad (37)$$

For the axi-symmetric problems suppose the impact pressure q is uniformly distributed over an annular area with inner radius a and outer radius b (see Fig. 4). Based on the 2D Flamant solution of a semi-infinite plate loaded by a concentrated vertical force P , the deflection at point M in the annular loaded area is:

$$u_z(x) = \frac{2q(1+\nu)(1-2\nu)}{\pi E_e(1-\nu)} \int_a^b \ln|r-\xi| d\xi \quad (38)$$

where the elastic constant is $E_e(1-\nu)/(1+\nu)(1-2\nu)$ for the axi-symmetric problems instead of the Young's modulus E_e for the plane stress problems (Timoshenko and Goodier, 1970, p. 109).

The force acting on an element including M is:

$$dF = 2\pi q r dr \quad (39)$$

The work done by the impact pressure is equal to:

$$\begin{aligned} W &= \int u_z dF \\ &= \frac{4q^2(1+\nu)(1-2\nu)}{E_e(1-\nu)} \int_a^b \int_a^b r \ln|r-\xi| d\xi dr \end{aligned} \quad (40)$$

where the integrand is singular at $r = \xi$. Thus the integral involves a the Cauchy principle value (see Appendix B).

The mass and kinetic energy of the annular liquid is:

$$m = \rho \cdot \frac{1}{4}\pi^2(a+b)d^2; \quad E = \frac{1}{2}mv^2 \quad (41)$$

where $d = b - a$, thus the impact pressure q is given by

$$\begin{aligned} q &= \frac{\pi}{4}(\mathbf{v}_r \cdot \mathbf{j}) \\ &\times \sqrt{\frac{k\rho E_e(1-\nu)(a+b)}{(1+\nu)(1-2\nu)[(a+b)(\ln d - 1/2) - d]}} \end{aligned} \quad (42)$$

Based on the Boussinesq solution Hertz created a famous contact theory and has applied the theory to solve a central collision problem of two elastic bodies. Experimental observations show that Hertz's theory based on a statically elastic case is also suitable to the impact analysis, as long as the material at contact area is elastic (Fluegge, 1962). For the impact analysis of the splashing liquid, the impact pressure is nearly uniform but not high concentrated as in the contact problem and the impact velocity is low, therefore, as a simplified theory, the solutions (37) and (42) can be applied to the HCDA analysis.

5. Computational implement

Based on the above theory a 2D axi-symmetric FEM computer code FRHCDA for the fluid-structure interaction analysis of HCDA in a LMFBR was developed.

In the code FRHCDA the fluid components are modeled by viscous incompressible fluid. Since large distortion and moving interfaces are involved, the arbitrary-Lagrange-Euler formulation expressed by Eqs. (10–26) are selected. The fluid domains include

the liquid sodium and the argon blanket are divided into axi-symmetrically quadratic elements. The structural components, include the roof, the reactor vessel and the inner vessel, are modeled by the bi-linear elastoplastic material and also divided into axi-symmetrically quadratic elements.

Dynamic properties of the fluid components and the structural components are quite different, so the coupled solving approach of whole fluid-structural system not only results in huge computational scale but also needs very fine time-steps. In the FRHCDA a split iterative solving approach is used, in which the fluid domain and the structural domain are dealt with alternatively, the coupling parameters (such as the displacement, the velocity and the pressure) are transferred through the interfaces in each iterated step.

The force boundary condition between the fluid and the vessel is

$$\mathbf{F}_f = -\mathbf{F}_s \quad (43)$$

The displacement boundary condition is

$$\mathbf{u}_f \cdot \mathbf{n}_f = \mathbf{u}_s \cdot \mathbf{n}_f \quad (44)$$

where the subscript f means the fluid components while the subscript s means the structural components. \mathbf{n}_f is the normal vector of the fluid boundary.

When a moved node of fluid (or solid) elements in an interface does not coincide with any node of solid (or fluid) elements in the same interface, the value of displacement and velocity (or pressure) transferred through the interface at this node are calculated by interpolation method.

For time integration of coupled dynamic analysis the Newmark method is applied.

The high-pressure gas bubble is modeled by the PPIG loading model introduced in Section 2. Set $\text{Const} = p_0 V_0$ and $n = 1$, Eq. (2) becomes:

$$pV = p_0 V_0 \quad (45)$$

where V_0 is the initial volume of the gas bubble, and if the total energy release is given the initial pressure of the gas bubble p_0 is got from Eq. (7) based on the “5% truncated criterion”.

The normal stresses in the liquid sodium are checked in each time step. If a liquid part is surrounded by the original free surface and the inner surface, on which

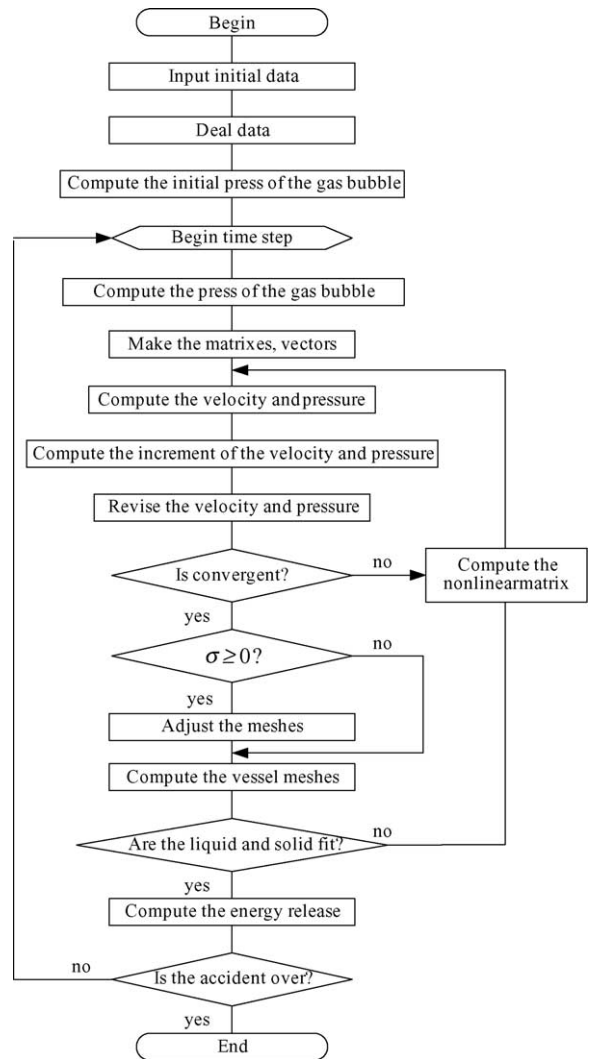


Fig. 5. The general flow chart of the code FRHCDA.

the normal stress is equal to or greater than zero, i.e. satisfies the separation criterion Eq. (27), a splashing part forms. The moving trace of the separated liquid part is described by the Newton’s law. The impact condition of the splashing liquid to the roof slab is given in Eq. (30). The impact pressure on the roof slab is computed with the Eq. (42) (2D axi-symmetric problems). We suppose the energy transfer coefficient $k = 0.95$.

The general flow chart of the code FRHCDA is shown in Fig. 5.

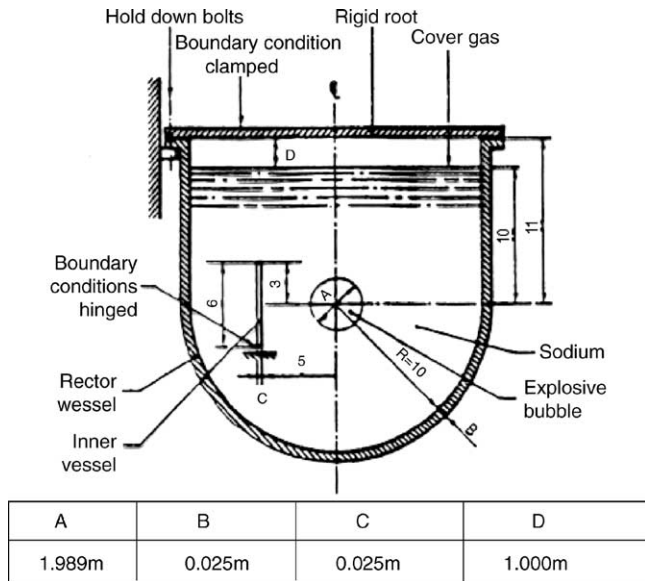


Fig. 6. The CONT benchmark problem.

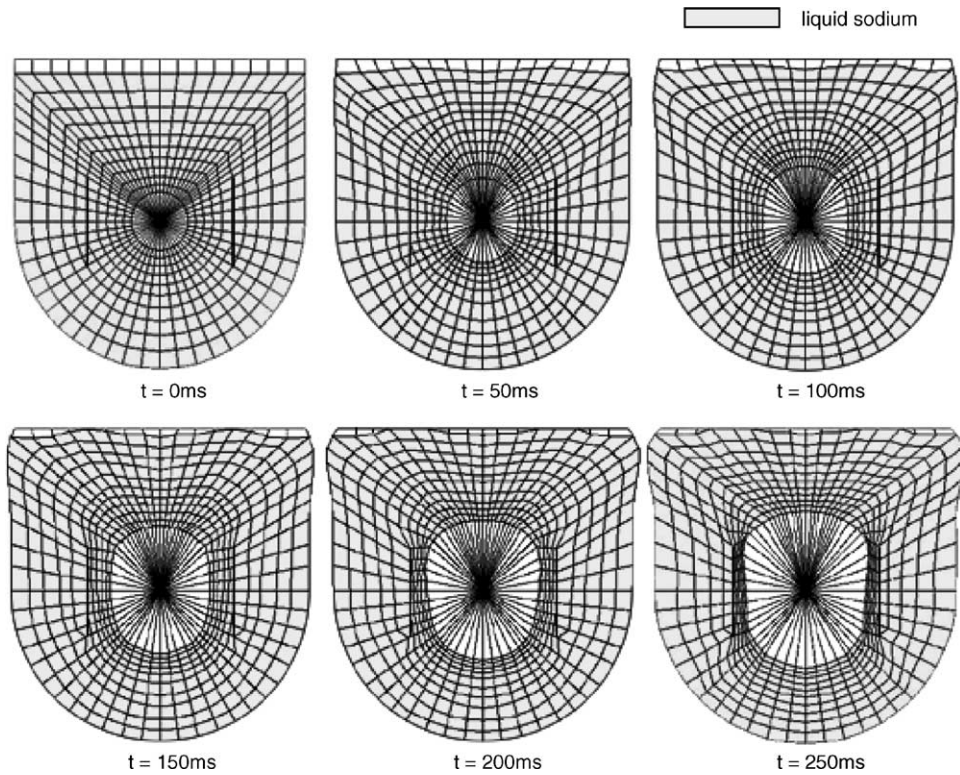


Fig. 7. Initial and deformed meshes (displacements magnified five times).

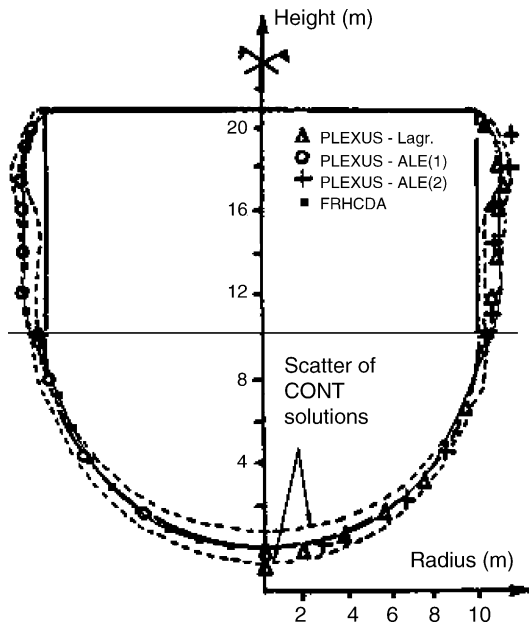


Fig. 8. Comparison of final deformed shapes calculated by various codes.

6. Benchmark problem

To check the effectiveness of FRHCDA, a CONT benchmark problem (Casadei et al., 1989) is calculated (see Fig. 6). The parameters of CONT problem are listed in Table 2. Fig. 7 shows the history of the mesh deformation. An initial mesh is drawn in the case of $t = 0$ ms. There are totally 282 elements and 320 nodes in the area of liquid sodium and argon blanket. Triangular elements are used in the area of gas bubble, which are totally 28 elements and 30 nodes. The time step is taken as 2 ms. The Lagrangian approach is adopted on the interface between the liquid sodium and the gas bubble, as well as on that between the liquid sodium

Table 2
The parameters of CONT problem

Parameter	Nominal value	Range
Bubble energy (MJ)	600	200–1000
Bubble pressure (MPa)	10	5–15
Cover gas gap (m)	1	0.2–1.8
Roof mass (MN/m ²)	100	50–150
Yield stress (MPa)	105	70–140
Plastic modulus (GPa)	3	1.5–4.5

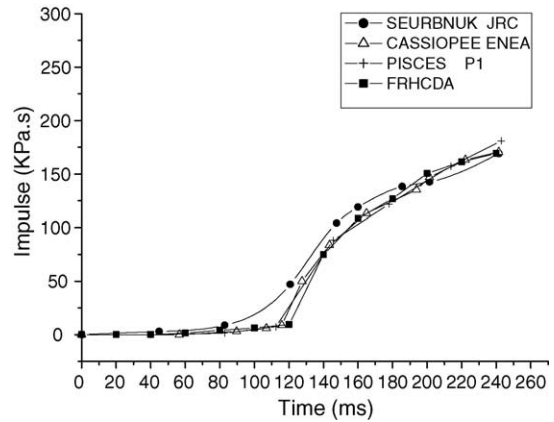


Fig. 9. Impulse vs. time.

and the argon blanket, while the ALE approach is used in the area of liquid sodium.

It is observed that the expanding speed of high-pressure gas bubble is lower than that of the high density explosive charge. The liquid sodium touches on the roof slab at the moment $t = 120$ ms.

A comparison of the deformed shape of reactor vessel calculated by our code and by the code PLEXUS (Casadei et al., 1989) is given in Fig. 8. All displacements in Fig. 7 are magnified five times. It can be seen

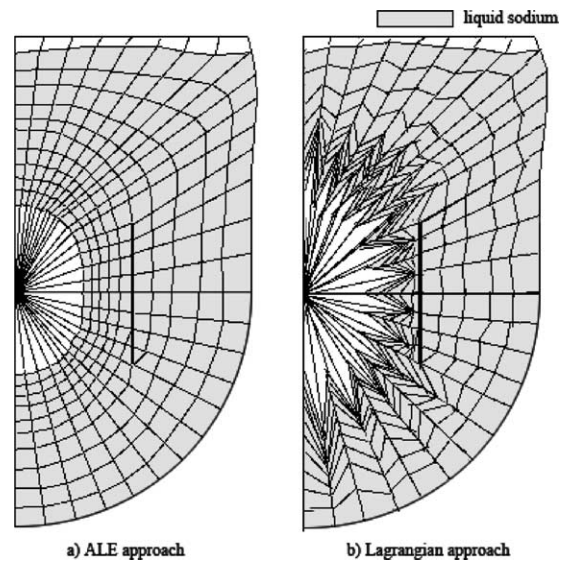


Fig. 10. deformed meshes of ALE and Lagrangian approaches at $t = 120$ ms.

that our results fall in the scatter range of the CONT solutions.

The maximal stress is 78.97 MPa on the external surface at central point of the vessel bottom.

The impulse on the roof slab is shown in Fig. 9. The rate of energy transfer k is taken as 0.95. It shows that our results are well within the existing results published in international journals (Balz and Dufresne, 1989).

The proportion of computing time in the first 20 time steps of the Lagrangian, the Eulerian and the ALE approach is 1:1.176:1.655. The ALE approach is a little expensive. However due to severe mesh distortion (see Fig. 10) the calculation of the Lagrangian approach diverges at $t = 124$ ms, and due to serious deformation of the free surface of liquid sodium, the Eulerian approach appears obvious error at $t = 158$ ms, but the ALE approach runs well from start to finish.

7. Conclusion

The following conclusions can be drawn:

- (1) The PPIG law is the most flexible loading model to simulate the HCDA process.
- (2) The ALE approach is successful to avoid severe mesh distortion and to deal with the moving interface. It is an ideal method for the HCDA analysis of a LMBFR.
- (3) An approach to treat with the liquid splash is proposed. Moreover a simplified analytical solution of the impact pressure on roof slab is derived. Computational results based on the researches in the present paper agree well with the existing results published on international journals.

Appendix A. Nomenclature

A, B, R_1, R_2, n	physical constants
\mathbf{a}	acceleration
E_e	Young's modulus
E	internal energy
\mathbf{F}	force vector
\mathbf{f}	force per unit mass
\mathbf{G}	gradient operator
\mathbf{g}	acceleration of gravity
\mathbf{K}	viscosity matrix

\mathbf{M}	mass matrix
m	mass of the liquid part
\mathbf{N}	non-linear vector of convection force
\mathbf{N}_v	shape function matrix of the velocity field
\mathbf{N}_p	shape function matrix of the pressure field
p	pressure
p_0	initial pressure
q	impact pressure
t	time
u_z	displacement
V	volume
V_0	initial volume
$V' V/V_0$	relative volume
\mathbf{v}	velocity
\mathbf{v}_0	initial velocity
\mathbf{v}_m	mesh velocity
W	total energy release

Greek letters

ϵ	strain
η	rate of volume
μ	kinematic viscosity
ν	Poisson's ratio
ρ	fluid density
σ	stress

Appendix B. Principle value of Cauchy integral

The general expression of Cauchy principle value of function $f(x)$ is:

$$\int_a^b f(x) dx = \lim_{\epsilon \rightarrow 0} \left[\int_a^{c-\epsilon} f(x) dx + \int_{c+\epsilon}^b f(x) dx \right] \tag{46}$$

where $a < c < b$, $\epsilon > 0$. Take the function $r \ln|r - \xi|$ instead of $f(x)$, we get

$$\begin{aligned} & \int_a^b r \ln|r - \xi| d\xi \\ &= r \left[\lim_{\epsilon \rightarrow 0} \int_a^{r-\epsilon} \ln(r - \xi) d\xi + \int_{r+\epsilon}^b \ln(\xi - r) d\xi \right] \\ &= r \left[\lim_{\epsilon \rightarrow 0} \left\{ -(r - \xi) \ln(r - \xi) - (r - \xi) \right\} \Big|_a^{r-\epsilon} \right. \\ & \quad \left. + [(\xi - r) \ln(\xi - r) - (\xi - r)] \Big|_{r+\epsilon}^b \right] \end{aligned}$$

$$\begin{aligned}
&= r \left[\lim_{\varepsilon \rightarrow 0} \{ -[(\varepsilon \ln \varepsilon - \varepsilon) - (r - a) \ln(r - a) \right. \\
&\quad \left. + (r - a)] + [(b - r) \ln(b - r) - (b - r) \right. \\
&\quad \left. - \varepsilon \ln \varepsilon + \varepsilon] \} \right] \\
&= r [(r - a) \ln(r - a) - (r - a) \\
&\quad + (b - r) \ln(b - r) - (b - r) + \lim_{\varepsilon \rightarrow 0} (\varepsilon - \varepsilon \ln \varepsilon)] \\
&= r(r - a) \ln(r - a) + r(b - r) \ln(b - r) \\
&\quad + r(a - b) \tag{47}
\end{aligned}$$

So Eq. (40) is

$$\begin{aligned}
W &= \frac{4q^2(1 + \nu)(1 - 2\nu)}{E_e(1 - \nu)} \int_a^b \int_a^b r \ln|r - \xi| d\xi dr \\
&= \frac{4q^2(1 + \nu)(1 - 2\nu)}{E_e(1 - \nu)} \int_a^b [r(r - a) \ln(r - a) \\
&\quad + r(b - r) \ln(b - r) + r(a - b)] dr \\
&= \frac{4q^2(1 + \nu)(1 - 2\nu)}{E_e(1 - \nu)} \\
&\quad \times \left[\frac{(a + b)}{2} \left(d^2 \ln d - \frac{d^2}{2} \right) - \frac{d^3}{2} \right] \tag{48}
\end{aligned}$$

where $d = b - a$

References

- Balz, W., Dufresne, J., 1989. Main results of activities performed by the CEC LMFBR Containment Expert Group. In: *Trans. SMiRT-10*, E, USA, pp. 269–279.
- Casadei, F., Daneri, A., Toselli, G., 1989. Use of PLEXUS as a LMFBR primary containment code for the CONT benchmark problem. In: *Trans. SMiRT-10*, E, USA, pp. 299–304.
- Cengel, Y.A., Boles, M.A., 2002. *Thermodynamics, An Engineering Approach*, fourth ed. McGraw-Hill Companies, Inc.
- Fluegge, W., 1962. *Handbook of Engineering Mechanics*. McGraw-Hill Book Company, Inc.
- Han, Y.C., 1980. Arbitrary Lagrangian–Eulerian method for transient fluid–structure interactions. *Nucl. Technol.* 51 (mid-December), 363–377.
- Harlow, F.H., Welch, J.E., 1965. Numerical calculations of time-dependent viscous incompressible flow of fluid with free surface. *Phys. Fluids* 8, 2182–2189.
- Hirt, C.W., Nichols, B.D., 1981. Volume of fluid (VOF) method for the dynamics of free boundaries. *J. Comp. Physics* 39, 201–225.
- Hoskin, N.E., Lancefield, M.J., 1978. The COVA programme for the validation of computer codes for fast reactor containment studies. *Nucl. Eng. Des.* 46, 17–46.
- Jiang, Bo-nan, 1998. *The Least-squares Finite Element Method*. Springer-Verlag.
- Kury, J.W., Hornig, H.C., Lee, E.L., McDonnel, J.L., Ornellas, D.L., Finger, M., Strange, F.M., Wilkins, M.L., 1965. *Proceedings of the Fourth Symposium on Detonation White Oak, USONR Report ACR-126*.
- Lepareux, M., Bung, H., Combesure, A., Aguilar, J., Flobert, J.F., 1993. Analysis of an HCDA in fast reactor with a multiphase and multicomponent behavior law. In: *Trans. SMiRT-12*, E, USA, pp. 197–202.
- Noh, C.E.L., 1964. A time-dependent two-space-dimensional coupled Eulerian–Lagrangian code. In: Alder, B., Fernbach, S., Rotenberg, M. (Eds.), *Methods in Computational Physics*, vol. 3. Academic Press, New York.
- Robbe, M.F., Lepareux, M., Treille, E., Cariou, Y., 2003. Numerical simulation of a hypothetical core disruptive accident in a small-scale model of a nuclear reactor. *Nucl. Eng. Des.* 223, 159–196.
- Timoshenko, S.P., Goodier, J.N., 1970. *Theory of Elasticity*. McGraw-Hill.
- Wang, C.-Y., 1980. Analysis of high-energy excursions using the implicit continuous-fluid Eulerian containment code (ICECO). *Nucl. Technol.* 51 (MID–DEC), 400–413.
- Wayne, R.Z., 1980. Events contributing to internal loading of secondary containment: an integrated approach. *Nucl. Technol.* 51 (MID–DEC), 476–488.
- Wenger, H.U., Smith, B.L., 1987. On the origin of the discrepancies between theory and experiment in the COVA series. In: *Trans SMiRT-9*, E, USA, pp. 339–344.
- Zhu, J., Sethian, J.A., 1992. Projection methods coupled to level set interface techniques. *J. Comput. Phys.* 102, 128–138.